


Cite this: *RSC Adv.*, 2020, 10, 29587

# Extraction and purification of $\epsilon$ -poly-L-lysine from fermentation broth using an ethanol/ammonium sulfate aqueous two-phase system combined with ultrafiltration†

Xusheng Chen, \* Wenjiao Diao, Yu Ma and Zhonggui Mao

$\epsilon$ -Poly-L-lysine ( $\epsilon$ -PL) serves as a natural food preservative and is manufactured mainly by extraction from microbial fermentation broth using ion-exchange chromatography. In order to develop an alternative purification strategy, an environmentally friendly alcohol/salt aqueous two-phase system (ATPS) was explored in this study for  $\epsilon$ -PL extraction. A study of the separation of  $\epsilon$ -PL in different alcohol/salt systems showed that ethanol/ammonium sulfate ATPS exhibited the highest  $\epsilon$ -PL partition coefficient and recovery ratio. Based on the phase diagram, the effect of phase composition on partition, and the removal of pigment and protein, an ATPS that was composed of 20% (w/w) ethanol and 20% (w/w) ammonium sulfate, with a feedstock at pH 9.5, was developed to extract  $\epsilon$ -PL from the fermentation broth. This achieved an  $\epsilon$ -PL recovery ratio of 96.15% with an  $\epsilon$ -PL purity of 40.23% after triplicate extractions. Subsequently, desalting by ultrafiltration led to a final  $\epsilon$ -PL product of 92.39% purity and 87.72% recovery. The ethanol/ammonium sulfate ATPS provides a new possibility for  $\epsilon$ -PL purification.

Received 12th May 2020

Accepted 27th July 2020

DOI: 10.1039/d0ra04245e

rsc.li/rsc-advances

## 1. Introduction

$\epsilon$ -Poly-L-lysine ( $\epsilon$ -PL) is composed of 25–35 L-lysine residues that are linked by adjacent  $\epsilon$ -amino and  $\alpha$ -carboxyl groups,<sup>1</sup> and can be produced by various *Streptomyces* spp., a few filamentous fungi and some *Bacilli* as a secondary metabolite.<sup>2,3</sup>  $\epsilon$ -PL and its derivatives have been used as preservatives, biodegradable fibers, hydrogels, drug carriers, biochip coatings in food and in the cosmetics and pharmaceutical fields.<sup>4</sup> Since the 1980s,  $\epsilon$ -PL has entered the commercial market as a natural food preservative in Japan, South Korea, the United States, and China, and it is manufactured industrially by aerobic fermentation using *Streptomyces albulus*.<sup>5</sup> As the  $\epsilon$ -PL market continues to grow at a rapid pace, the development of an efficient bio-separation process is critical for  $\epsilon$ -PL production, and this would help to significantly reduce the cost of  $\epsilon$ -PL production.

Based on a search of the literature, an initial  $\epsilon$ -PL purification scheme including cation ion-exchange adsorption, activated-carbon decoloration and organic-solvent precipitation was developed to identify the  $\epsilon$ -PL chemical structure in 1981.<sup>1</sup> Using this approach, Bankar *et al.* purified  $\epsilon$ -PL from fermentation broth that contained 2 g L<sup>-1</sup>  $\epsilon$ -PL, with a purity of 97.58% and a recovery ratio of 90.42%.<sup>6</sup> Zhu *et al.* evaluated the  $\epsilon$ -PL

adsorption performance of HZB-3B (strong cation) and D155 (weak cation) resins and optimized the adsorption and desorption conditions to achieve a desorption efficiency of 97.57% and a recovery ratio of 94.49%.<sup>7</sup> Chen *et al.* employed an Amberlite IRC-50 ion-exchange resin, a SX-8 macroporous adsorption resin and Sephadex G-25 gel column chromatography to purify  $\epsilon$ -PL from a culture of *S. ahyscopicus*, and this was used for its chemical structure identification.<sup>8</sup> In previous studies, we developed a potential industrial scheme for  $\epsilon$ -PL separation and purification from fermentation broth, including mycelia removal by flocculation, protein removal by 30 kDa ultrafiltration, ion-exchange adsorption, decolorization with a macroporous resin and desalting by 1 kDa ultrafiltration. A 90.2% purity and 75% recovery were achieved.<sup>9</sup> In order to improve the purity of  $\epsilon$ -PL and its efficiency, we optimized the ion form of a cation ion-exchange resin and found that NH<sub>4</sub><sup>+</sup> was the optimal ion form of the cation resin that was used for  $\epsilon$ -PL extraction. The  $\epsilon$ -PL purity was improved to 97.10% with a recovery ratio of 66.01%.<sup>10</sup> Thus, the developed scheme based on an ion-exchange operation could achieve  $\epsilon$ -PL purification from a fermentation broth with a high purity and acceptable recovery ratio. However, these bioseparation processes are complicated, and a large volume of saline wastewater is produced during the ion-exchange operation, increasing the economic and environmental problems. Therefore, it is necessary to develop an alternative extraction technology for  $\epsilon$ -PL purification. Recently, Katano *et al.* proposed a precipitation method to separate and purify  $\epsilon$ -PL from culture broth using the

The Key Laboratory of Industrial Biotechnology, Ministry of Education, School of Biotechnology, Jiangnan University, Wuxi 214122, China. E-mail: chenxs@jiangnan.edu.cn; Fax: +86 510 85918296; Tel: +86 510 85918296

† Electronic supplementary information (ESI) available. See DOI: 10.1039/d0ra04245e



tetraphenylborate anion, and recovered 95%  $\epsilon$ -PL from a 100  $\mu$ L culture.<sup>11</sup> Furthermore, they developed a yellow anionic dye, the dipicrylamine anion, to precipitate polycationic  $\epsilon$ -PL.<sup>12</sup> Moreover, metal-chelate affinity precipitation was used for  $\epsilon$ -PL purification, and this afforded 98.42% recovery with electrophoretic purity.<sup>13</sup> Unfortunately, these methods are only suitable for research purposes and are unsuitable for industrial application in terms of cost and food safety. Thus, it is necessary to continue to discover an efficient, high food safety and inexpensive strategy for  $\epsilon$ -PL purification.

An aqueous two-phase system (ATPS) comprises two immiscible aqueous-rich phases, which are formed by mixing phase-forming component(s) above a critical concentration.<sup>14</sup> Typical ATPS types are based on polymer/polymer systems and polymer/salt systems. The major drawbacks that limit the practical application of both ATPSs are the high cost of some phase-forming polymers, the high viscosity of the polymer phase, the slow phase segregation, the difficulty in product isolation from a polymer-rich phase and complications in the recycling of phase components.<sup>15</sup> In recent years, the alcohol/salt ATPS has become a promising and sustainable variant of the ATPS that has garnered popularity in the purification of biomolecules. This type of ATPS allows for easier recovery of the target compound by alcohol removal using an evaporation method, compared with a conventional ATPS.<sup>16</sup> The method also produces less pollution and has a low cost, because alcohol and salt can be recycled *via* distillation and crystallization, respectively. For example, Lo *et al.* developed an alcohol/salt ATPS comprising 1-propanol and tripotassium citrate that was used for green fluorescent protein purification from the culture of recombinant *Escherichia coli*, yielding an average green fluorescent protein purification factor of 11.34 and a 75.7% of EGFP recovery ratio.<sup>17</sup> Mathiazakan *et al.* reported that lipase could be recovered and purified from the fermentation broth of *Burkholderia cepacia* using a 1-propanol and ammonium sulphate ATPS combined with solvent sublation on a pilot scale, achieving a purification factor of 12.2, a separation efficiency of 93% and a selectivity of 40.<sup>18</sup> However, no report currently exists on  $\epsilon$ -PL purification using an alcohol/salt ATPS.

In this study, the separation of  $\epsilon$ -PL in different alcohol/salt systems was investigated. An ethanol/ammonium sulfate system was chosen to separate  $\epsilon$ -PL from fermentation broth because of the low cost and facile recycling of the solvent and salt. The influence of the phase-forming components on the separation of  $\epsilon$ -PL and the removal of proteins and pigments was also investigated. The effect of multi-stage extraction and desalting on the purity of  $\epsilon$ -PL and its recovery were also evaluated. This study is the first report that presents a simple and effective method to extract  $\epsilon$ -PL from fermentation broth directly using an aqueous two-phase system.

## 2. Results and discussion

### 2.1 Partition of $\epsilon$ -PL in different alcohol/salt systems

The separations of  $\epsilon$ -PL in different alcohol/salt systems are shown in Table 1. Methanol could not form an ATPS with all the salts tested. Similarly, sodium phosphate could not form

Table 1 Separation of  $\epsilon$ -PL in different alcohol/salt systems<sup>a</sup>

		(NH <sub>4</sub> ) <sub>2</sub> SO <sub>4</sub>	NaH <sub>2</sub> PO <sub>4</sub>	KCl	NaCl	Na <sub>3</sub> PO <sub>4</sub>
Methanol	<i>K</i>	—	—	—	—	—
	<i>Y</i> (%)	—	—	—	—	—
Ethanol	<i>K</i>	18.27	10.21	—	—	—
	<i>Y</i> (%)	97.89	81.23	—	—	—
Acetone	<i>K</i>	1.52	1.21	1.03	—	—
	<i>Y</i> (%)	53.26	48.34	46.32	—	—
Ethyl acetate	<i>K</i>	0.19	0.07	—	0.06	—
	<i>Y</i> (%)	18.46	5.21	—	1.12	—

<sup>a</sup> —, homophase.

a phase separation with all the tested alcohols. In the ATPSs that were formed, the partition coefficient (*K*) and recovery ratio (*Y*) of  $\epsilon$ -PL in ethanol/ammonium sulfate and ethanol/sodium dihydrogen phosphate ATPSs were higher than in other investigated alcohol/salt systems. In particular, the *K* and *Y* values in the ethanol/ammonium sulfate ATPS were the highest at 18.27% and 97.89%, respectively. The *K* and *Y* values in the ethanol/sodium dihydrogen phosphate ATPS were 10.21% and 81.23%, respectively. However, the *K* values in the other ATPSs ranged from 0.06–1.52, with *Y* ranging from 1.12% to 53.26%, which are significantly lower than those of the ethanol/ammonium sulfate or ethanol/sodium dihydrogen phosphate ATPSs. The reason why  $\epsilon$ -PL can be extracted by an ATPS remains unclear, but one possible reason could be the hydrophilicity of  $\epsilon$ -PL and that of the solvent. In the ATPS, the hydrated ions of the salts, especially the hydrated anions with H<sub>3</sub>O<sup>+</sup>, can bind to water molecules from the solution. The multivalent anion can bind to more water molecules than the monovalent anion.<sup>19</sup> Therefore, sulfate and dihydrogen phosphate can promote  $\epsilon$ -PL to form a new phase from the feedstock. However, phosphate did not yield a phase separation because of its high hydrophilicity. Other salts (KCl and NaCl) that contain monovalent charge anions alone were less efficient at binding water molecules. A stronger solvent polarity resulted in increased bound water. Thus, it is easy to understand that the extraction of  $\epsilon$ -PL by an ethanol/salt system is superior to that of other organic solvent/salt systems. However, it is difficult for the investigated salts to promote methanol to form an ATPS because of the sufficient affinity between water and methanol.

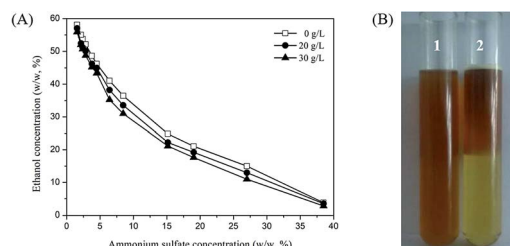


Fig. 1 Phase diagram of the ethanol/ammonium sulfate ATPS in deionized water and  $\epsilon$ -PL feedstock (A), and the state of ATPS extraction of the  $\epsilon$ -PL feedstock ((1),  $\epsilon$ -PL feedstock; (2) ATPS extraction) (B). The experiments were performed in triplicate.



Based on the partition coefficient, the recovery ratio and the cost of salt, the ethanol/ammonium sulfate ATPS was chosen for  $\epsilon$ -PL extraction.

## 2.2 Phase diagram of the ethanol/ammonium sulfate ATPS in the $\epsilon$ -PL feedstock

The phase diagram of the ethanol/ammonium sulfate ATPS with different concentrations of  $\epsilon$ -PL is shown in Fig. 1. Without  $\epsilon$ -PL (deionized water), two extreme points of phase formation were chosen; one point occurred at 1.6% (w/w) ammonium sulfate and 58.1% (w/w) ethanol, and the other occurred at 38.5% (w/w) ammonium sulfate and 3.8% (w/w) ethanol, which is consistent with the results of a previous study.<sup>19</sup> In the  $\epsilon$ -PL feedstock, the presence of  $\epsilon$ -PL did not change the binodal curve in deionized water, but the concentration of ethanol at the phase-forming point at each  $\epsilon$ -PL concentration was lower than that in deionized water at the same concentration of ammonium sulfate. A binodal curve closer to the origin in the phase diagram implies that ATPS formation could be achieved at lower concentrations of the phase-forming components.<sup>20</sup> The displacement of binodal curves from the origin of the phase diagram was in the order:  $30 \text{ g L}^{-1} < 20 \text{ g L}^{-1} < 0 \text{ g L}^{-1}$ , indicating that  $\epsilon$ -PL benefited ethanol/ammonium sulfate ATPS formation.  $\epsilon$ -PL was partitioned in the top phase of the ethanol/ammonium sulfate ATPS (ethanol phase) and was recovered easily by removing ethanol *via* evaporation (Fig. 1B). Most  $\epsilon$ -PL-producing strains could achieve  $\epsilon$ -PL concentrations of approximately  $30 \text{ g L}^{-1}$  in the fermentation broth.<sup>21</sup> Therefore, the ethanol/ammonium sulfate ATPS was developed directly in the  $\epsilon$ -PL feedstock ( $30 \text{ g L}^{-1}$ ) for  $\epsilon$ -PL purification, and this is beneficial for industrial applications and process economics.

## 2.3 Optimization of the ethanol/ammonium sulfate ATPS for $\epsilon$ -PL extraction

To develop the ethanol/ammonium sulfate ATPS in the  $\epsilon$ -PL feedstock, the separations of  $\epsilon$ -PL in the ethanol/ammonium sulfate ATPSs were investigated at varying ammonium sulfate and ethanol concentrations, and the pH of the  $\epsilon$ -PL feedstock was varied. The results are shown in Fig. 2.

As shown in Fig. 2A, the partition coefficient of  $\epsilon$ -PL in the ethanol/ammonium sulfate ATPS decreased with an increase in ammonium sulfate concentration from 20% (w/w) to 23.3% (w/w), but the coefficient increased when the ammonium sulfate concentration exceeded 23.3% (w/w). The recovery efficiency of an alcohol/salt ATPS for biotechnological product purification is dependent on the salting-out mechanism.<sup>22</sup> In the ethanol/ammonium sulfate ATPS, when the concentration of ammonium sulfate was increased in the system (from 20% to 23.3%), more water molecules in the top phase were transferred to the bottom phase and combined with ammonium and sulfate ions, resulting in a decrease of  $\epsilon$ -PL solubility in the top phase. However, when the concentration of ammonium sulfate was increased further (from 23.3% to 26.7%), the salting-out effect occurred in the bottom phase, repelling the  $\epsilon$ -PL that was dissolved in the top phase and again increasing the  $\epsilon$ -PL partition coefficient. As the  $\epsilon$ -PL recovery ratio is related closely to the  $\epsilon$ -PL partition coefficient, it exhibited the same trend as the  $\epsilon$ -PL partition coefficients. As shown in Fig. 2B, the decolorization and protein removal ratios improved steadily with an increase in ammonium sulfate concentration, reaching the highest values of 40.1% and 43.2%, respectively, at an ammonium sulfate concentration of 26.7% (w/w). Based on the  $\epsilon$ -PL recovery efficiency, 20% (w/w) ammonium sulfate was chosen for the ethanol/ammonium sulfate ATPS.

Interestingly, as shown in Fig. 2C, the partition coefficients of  $\epsilon$ -PL in the ATPS during ethanol concentration optimization exhibited the same trend as that of ammonium sulfate optimization (Fig. 2A). However, the reasons for this are different. It has been reported that an increase in ethanol concentration in the top phase of the ATPS causes gradual dehydration of the top phase and favours the partitioning of compounds to the bottom phase.<sup>23</sup> However, when the ethanol concentration increases further in the top phase, an increased number of water molecules in the bottom phase are transferred to the top phase, due to the dehydration effect of ethanol, resulting in the bottom phase producing a salting-out effect and causing the  $\epsilon$ -PL partition coefficient to improve (Fig. 2C). The  $\epsilon$ -PL recovery ratios showed the same trend as the  $\epsilon$ -PL partition coefficients, because the  $\epsilon$ -PL recovery ratio is related closely to the  $\epsilon$ -PL partition coefficient (Fig. 2C). As shown in Fig. 2D, the decolorization ratio increased steadily with an increase in ethanol concentration, but the protein removal ratio decreased steadily, possibly due to the protein and pigment having opposite polarity. Thus, 20% (w/w) ethanol was chosen for the ethanol/ammonium sulfate ATPS in terms of  $\epsilon$ -PL recovery ratio.

$\epsilon$ -PL is an amphoteric compound with an isoelectric point of  $\sim 9.0$ ,<sup>24</sup> indicating that it is positively charged below pH 9.0 and

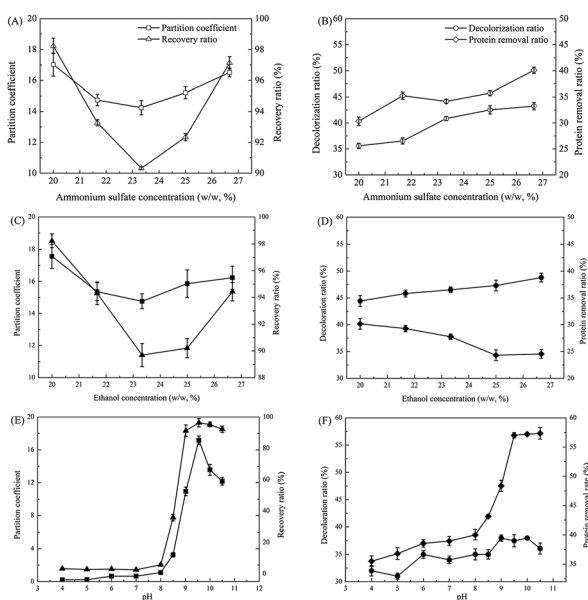


Fig. 2 Effect of ammonium sulfate (A and B), ethanol (C and D) and pH (E and F) on the  $\epsilon$ -PL partition coefficient,  $\epsilon$ -PL recovery ratio, decolorization ratio and protein removal ratio in the ethanol/ammonium sulfate ATPS. The experiments were performed in triplicate and error bars indicate the standard deviations.

Table 2 Multistage extractions of  $\epsilon$ -PL using the ethanol/ammonium sulfate ATPS

Extraction time	$\epsilon$ -PL partition coefficient	Volume ratio (top/bottom)	$\epsilon$ -PL recovery ratio (%)	Protein removal ratio (%)	Decolorization ratio (%)	$\epsilon$ -PL purity (%)
0	—	—	100	0.00	0.00	$19.93 \pm 1.61$
1	$20.01 \pm 1.21$	$1.21 \pm 0.54$	$98.11 \pm 0.41$	$57.23 \pm 1.12$	$37.68 \pm 1.09$	$28.26 \pm 1.57$
2	$18.85 \pm 1.56$	$1.02 \pm 0.12$	$96.21 \pm 0.15$	$63.27 \pm 1.03$	$40.19 \pm 0.56$	$34.67 \pm 0.73$
3	$18.36 \pm 2.01$	$0.91 \pm 0.34$	$96.15 \pm 0.23$	$85.66 \pm 1.04$	$58.98 \pm 1.25$	$38.91 \pm 2.02$
4	$18.01 \pm 1.76$	$0.92 \pm 0.21$	$92.01 \pm 0.30$	$86.56 \pm 1.43$	$60.01 \pm 0.98$	$40.23 \pm 1.21$

negatively charged above pH 9.0. When the pH is below 8.0, most of the  $\epsilon$ -PL exists in its cation form, which has a high solubility in the bottom phase. However, when the pH is increased from 8.0 to 9.0, the net electrical charge of  $\epsilon$ -PL approaches zero, which increases the solubility of  $\epsilon$ -PL in the top phase and results in a rapid increase in the  $\epsilon$ -PL partition coefficient. When the pH is higher than 9.0, the negatively charged  $\epsilon$ -PL shows improved solubility in the bottom phase again, decreasing the  $\epsilon$ -PL partition coefficient (Fig. 2E). As a result, the highest  $\epsilon$ -PL partition coefficient of 17.2 was achieved at pH 9.5. When the pH of the system exceeded 10.5,  $\text{NH}_3$  escaped from the system (the smell was noticeable during the experiment) due to the combination of  $\text{NH}_4^+$  and  $\text{OH}^-$  under alkali conditions, resulting in an unstable system. Similarly, the  $\epsilon$ -PL recovery ratio showed the same trend as the  $\epsilon$ -PL partition coefficients during the ethanol and ammonium sulfate optimization processes. In addition, as shown in Fig. 2F, decolorization and protein removal ratios increased with an increase of pH, achieving the highest values of 37.5% and 57.0%, respectively, at pH 9.5. The protein removal ratio was affected significantly by the increase in pH, possibly because the pH affected the charge-state of the protein, and this affected the protein removal.<sup>15</sup> Therefore, a feedstock pH of 9.5 was chosen for the ethanol/ammonium sulfate ATPS.

By combining the above results, the highest partition coefficient of  $\epsilon$ -PL was observed in the ethanol/ammonium sulfate ATPS that contained 20% ammonium sulfate and 20% ethanol at a feedstock pH of 9.5, and this yielded a partition coefficient and  $\epsilon$ -PL recovery ratio of 17.17 and 96.36%, respectively (Fig. 2E). The maximum decolorization and protein removal ratios were 37.5% and 57.0% (Fig. 2F), respectively. As a result, this system was selected for the extraction of  $\epsilon$ -PL from the feedstock.

#### 2.4 Multistage extraction of $\epsilon$ -PL from fermentation broth using the ethanol/ammonium sulfate ATPS

To maximize the ability of the ethanol/ammonium sulfate ATPS to extract  $\epsilon$ -PL and remove impurities, multistage ATPS extractions were performed. As shown in Table 2, the  $\epsilon$ -PL partition coefficient, volume ratio and  $\epsilon$ -PL recovery ratio decreased with an increase in extraction time. However, the  $\epsilon$ -PL purity, protein removal ratio and decolorization ratio improved with an increase in extraction time, indicating that the ethanol/ammonium sulfate ATPS had a high  $\epsilon$ -PL extraction efficiency. When the  $\epsilon$ -PL feedstock was extracted by the ethanol/

ammonium sulfate ATPS three times, the  $\epsilon$ -PL purity was enhanced by 95.2% and 37.7% compared with that in the feedstock and after a single extraction, respectively. The  $\epsilon$ -PL recovery ratio was  $96.15\% \pm 0.23\%$  in the third extraction, and this was 2% lower than the ratio in the single extraction. In addition, 58.98% pigment and 85.66% impurity protein were removed after the third extraction. When the  $\epsilon$ -PL feedstock was subjected to a fourth ATPS extraction, the protein removal ratio, decolorization ratio and  $\epsilon$ -PL purity did not improve visibly, compared with the third extraction, and the  $\epsilon$ -PL recovery ratio decreased from 96.15% to 92.01%.

As shown in Table 2, the apparent  $\epsilon$ -PL purity did not improve as expected, regardless of the extraction numbers, because the ammonium sulfate dissolved in the ethanol phase,<sup>14</sup> and this resulted in a decrease in the apparent  $\epsilon$ -PL purity. However, the  $\epsilon$ -PL peak gradually occupied the main component in the top phase of the ATPS with an increase in the extraction number through high-performance liquid chromatography (HPLC) analysis (Fig. 3). Impurities were removed gradually through the bottom phase of the ATPS (ESI Fig. 1†), indicating that the real  $\epsilon$ -PL purity would improve significantly in each extraction.  $\epsilon$ -PL appeared in the bottom phase from the third extraction, and this reflects that the extraction ability of the top phase for  $\epsilon$ -PL decreases with an increase in extraction number. Therefore, a triplicate extraction is the best choice for  $\epsilon$ -PL purification from feedstock using the ethanol/ammonium sulfate ATPS.

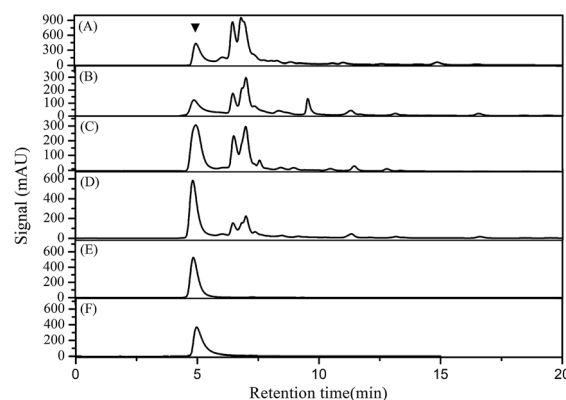
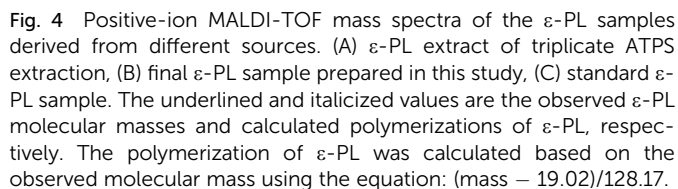


Fig. 3 HPLC chromatograms of  $\epsilon$ -PL analysis for the top phase during the ethanol/ammonium sulfate ATPS extraction. (A)  $\epsilon$ -PL feedstock, (B) first ATPS extraction, (C) second ATPS extraction, (D) third ATPS extraction, (E) final  $\epsilon$ -PL sample after ultrafiltration treatment, (F) the standard  $\epsilon$ -PL sample. The triangle indicates  $\epsilon$ -PL.





To remove ammonium sulfate from the ATPS extract and to evaluate the real  $\varepsilon$ -PL purity after three successive ATPS extractions, cross-flow ultrafiltration with a molecular cut-off weight of 1 kD was used.<sup>25</sup> After the ultrafiltration operation, the  $\varepsilon$ -PL purity increased from 38.91% (the third ATPS extract) to 92.78%, which was a 1.38-fold enhancement. Impurities with a retention time between 6.5 min and 7.5 min were removed, and the final  $\varepsilon$ -PL sample showed a single peak in the HPLC chromatogram (Fig. 3E), indicating that ultrafiltration removed ammonium sulfate and eliminated small-molecule impurities. The ultrafiltration operation recovered 91.24%  $\varepsilon$ -PL from the ATPS extract.

As a natural food preservative, the antimicrobial activity of  $\epsilon$ -PL is dependent mainly on its polymerization degree.<sup>9</sup> Thus, the effect of successive ATPS extractions on the polymerization degree of  $\epsilon$ -PL was investigated.  $\epsilon$ -PL samples were extracted three times using the ATPS, were desalted by ultrafiltration and analysed using MALDI-TOF-MS, and the results are shown in Fig. 4. The two  $\epsilon$ -PL samples had similar mass spectra compared with those of the standard  $\epsilon$ -PL sample, and they maintained the same characteristic as our previous results,<sup>9,25</sup> indicating that there was no negative effect of ATPS extraction on the polymerization degree of  $\epsilon$ -PL. The difference between the maximum polymerization degree between the  $\epsilon$ -PL samples prepared in this study and the standard  $\epsilon$ -PL sample lies in the  $\epsilon$ -PL-producing strain being different.<sup>9</sup>

### 3. Conclusions

$\epsilon$ -PL was extracted by an alcohol/salt ATPS from the feedstock for the first time. By investigating the separation of  $\epsilon$ -PL in different alcohol/salt systems, we found that the ethanol/ammonium sulfate ATPS exhibited the highest  $\epsilon$ -PL partition coefficient and recovery ratio. Based on the conditions of the ethanol/ammonium sulfate ATPS optimization, the optimum ATPS condition was 20% (w/w) ethanol with 20% (w/w) ammonium sulfate with the feedstock at pH 9.5. Triplicate ATPS

extraction yielded a partition coefficient of 18.36 with 96.15%  $\epsilon$ -PL recovery and 38.91%  $\epsilon$ -PL purity. After desalting treatment by ultrafiltration, the final  $\epsilon$ -PL had 92.39% purity and 87.72% recovery. These results show that the ethanol/ammonium sulfate ATPS could be used as an alternative for  $\epsilon$ -PL purification, but improvements in  $\epsilon$ -PL purity still require further study.

## 4. Experimental

Methanol, ethanol, acetone, ethyl acetate,  $(\text{NH}_4)_2\text{SO}_4$ ,  $\text{NaH}_2\text{PO}_4$ ,  $\text{KCl}$ ,  $\text{NaCl}$ ,  $\text{Na}_3\text{PO}_4$  and  $\text{Na}_2\text{SO}_4$  were purchased from Sino-pharm Chemical Reagent Co. Ltd (Shanghai, China). Acetonitrile was obtained from TEDIA (Fairfield, Ohio, USA). A protein assay kit was obtained from Bio-Rad (California, USA). The standard  $\epsilon$ -PL sample with a purity of 98.5% was provided by Jiangsu Yiming Biological Co., Ltd (Jiangsu, China). All chemicals used in this study were of analytical grade.

The  $\epsilon$ -PL-containing fermentation broth was prepared by *Streptomyces albulus* M-Z18, as described in our previous study.<sup>9</sup> The mycelia of the fermentation broth were removed by centrifugation at 14 000  $g$  for 20 min, and the supernatant containing  $\epsilon$ -PL with a concentration of 30 g L<sup>-1</sup> was used as the  $\epsilon$ -PL feedstock in this study.

The partition experiments were conducted by adding 6.0 g of different organic solvents to 18.0 g of  $\epsilon$ -PL feedstock containing 6.0 g of different salts in a graduated tube. The mixtures were vortexed for 5 min and then allowed to stand for 2 h. The concentrations of  $\epsilon$ -PL in the top and bottom phases were analysed by the methyl orange method. The partition coefficient ( $K$ ) of  $\epsilon$ -PL was defined as the ratio of the concentration of  $\epsilon$ -PL in the top phase to that in the bottom phase. The recovery ratio ( $Y$ ) of  $\epsilon$ -PL was defined as the weight of  $\epsilon$ -PL partitioned in the top phase to the total weight of  $\epsilon$ -PL in the feedstock.

Turbidity titration was used to obtain the phase diagrams of the ethanol/ammonium sulfate ATPS in deionized water.<sup>26</sup> Different weights of ammonium sulfate were dissolved in deionized water and added into test tubes. Then, ethanol was added dropwise to each test tube placed on an analytical balance to measure the weight of the added ethanol. After each droplet, the mixture was shaken for 2 min on a vortex mixer. When the mixture became turbid, two phases were still present in the system. However, when one more drop of ethanol was added, the turbidity disappeared and this point was considered to be the turbidity point. The total weight of ethanol added was measured precisely. The concentrations of ethanol and ammonium sulfate at different turbidity points were calculated using the following equations, and the phase diagram curve was plotted.

$$W_1 = \frac{m_1}{m_1 + m_2 + m_3}$$

$$W_2 = \frac{m_2}{m_1 + m_2 + m_3}$$

$W_1$  and  $W_2$  represent the mass fractions of ethanol and ammonium sulfate, respectively.  $m_1$ ,  $m_2$  and  $m_3$  represent the weights of ethanol, ammonium sulfate, and deionized water, respectively.

Phase diagrams of the ethanol/ammonium sulfate ATPS in the feedstocks with  $\epsilon$ -PL concentrations of 20 and 30 g L<sup>-1</sup> were investigated by adding various weights of solid ammonium sulfate. The turbidity points for each feedstock were then determined by adding ethanol dropwise, as described above.

#### 4.5 Partition behavior of $\epsilon$ -PL in the ethanol/ammonium sulfate ATPS

To investigate the effect of (NH<sub>4</sub>)<sub>2</sub>SO<sub>4</sub> and ethanol on the  $\epsilon$ -PL partition behaviour, 20–27% (w/w) of solid (NH<sub>4</sub>)<sub>2</sub>SO<sub>4</sub> and 20–27% (w/w) ethanol were added into 18.0 g of  $\epsilon$ -PL feedstock (pH 9.5) with an  $\epsilon$ -PL concentration of 30 g L<sup>-1</sup> to form the ATPS. Furthermore, in order to evaluate the effect of pH on the  $\epsilon$ -PL partition behaviour, several 18.0 g  $\epsilon$ -PL feedstocks (30 g L<sup>-1</sup>) were first adjusted to different pH values ranging from 4.0 to 10.5 by 2.0 M acid/alkali solutions, and then optimal weights of (NH<sub>4</sub>)<sub>2</sub>SO<sub>4</sub> and ethanol were added to each  $\epsilon$ -PL feedstock, forming the ATPS. The mixture was vortexed for 5 min and held for 2 h at room temperature (ca. 20 °C). The  $\epsilon$ -PL partition coefficient and recovery ratio were defined, as shown in Section 4.3. The removal mass ratio of protein was defined as the ratio of the weight of protein partitioned in the bottom phase to the total protein in the  $\epsilon$ -PL feedstock. The pigment concentration was expressed as the absorbance of the sample at 410 nm on a spectrophotometer. To make sure that the absorbance was carried out in the range of 0.2–0.6, deionized water was used to dilute the samples. The decolorization ratio was calculated as follows:

$$\text{Decolorization ratio (\%)} = \frac{A_1 \times V_1}{A_0 \times V_0} \times 100\%$$

where  $A_0$  and  $A_1$  are the absorbance values of the  $\epsilon$ -PL feedstock and the bottom phase, respectively.  $V_0$  and  $V_1$  (mL) are the volumes of the  $\epsilon$ -PL feedstock and the bottom phase, respectively.

#### 4.6 Multistage ethanol/ammonium sulfate ATPS extraction

Under the optimal conditions, the first extraction was carried out with a total weight of the ATPS at 300.0 g. Then, the top phase was transferred to a fresh bottom phase that had the same composition and volume as the first extraction. The mixture was stirred for 5 min to equilibrate and was given 2.0 h for phase separation. Similarly, the third and fourth extractions were carried out as described above. The volume ratio was defined as the ratio of the top phase volume to that of the bottom phase. The purity of  $\epsilon$ -PL in the top phase was calculated as follows:

$$\epsilon\text{-PL purity (\%)} = \frac{C \times V}{m} \times 100\%$$

where  $C$  is the  $\epsilon$ -PL concentration in the top phase determined by the methyl orange method,  $V$  is the volume of the top phase, and  $m$  is the dry weight of the ATPS extract, which is the top phase after evaporation at 40 °C and –0.08 MPa.

#### 4.7 Further purification of the ATPS extract

To remove ammonium sulfate from the ATPS extract, the top phase of the third ATPS extraction was concentrated by rotary evaporation at 40 °C and –0.08 MPa to remove ethanol. Then, the concentrate was diluted with deionized water and subjected to a cross-flow ultrafiltration system (Pellicon 2 mini, Merck Millipore, MA, USA), equipped with a regenerated cellulose membrane (0.1 m<sup>2</sup>) with a molecular cut-off weight of 1 kD, and drying as described in our previous study.<sup>9</sup>

#### 4.8 Analytical methods

The  $\epsilon$ -PL concentrations in the feedstock and top/bottom phases were determined using the methyl orange method.<sup>27</sup> However, the final  $\epsilon$ -PL sample and the process of ATPS extraction were analysed by HPLC.<sup>28</sup> In brief, a TSK gel ODS-120T column ( $\Phi$  4.6 × 250 mm, 5  $\mu$ m, Tokyo, Japan) and a wavelength of 215 nm were used at 25 °C. The mobile phase consisted of 8% acetonitrile in deionized water containing 1.7 g L<sup>-1</sup> K<sub>2</sub>HPO<sub>4</sub> and 1.42 g L<sup>-1</sup> Na<sub>2</sub>SO<sub>4</sub> (pH 3.4). The protein concentration and pigment absorbance were determined following procedures from a previous study.<sup>29</sup> Matrix-assisted-laser-desorption-ionization (MALDI)-time-of-flight (TOF)/mass spectrometry (MS) (ultrafleXtreme, Bruker Daltonics Inc., MA, USA) was used to analyse the distribution of  $\epsilon$ -PL molecular masses, and 2,5-dihydroxybenzoic acid was used as the matrix.<sup>30</sup>

## Conflicts of interest

There are no conflicts to declare.

## Acknowledgements

This work was financially supported by the Natural Science Foundation of China (31671846), the Natural Science Foundation of Jiangsu Province (BK20191332), the National First-Class Discipline Program of Light Industry Technology and Engineering (LITE2018-27), and the Program of Introducing Talents of Discipline to Universities (111-2-06).

## References

- 1 S. Shima and H. Sakai, *Agric. Biol. Chem.*, 1981, **45**, 2503–2508.
- 2 M. Nishikawa and K. Ogawa, *Appl. Environ. Microbiol.*, 2002, **68**, 3575–3581.
- 3 N. A. El-Sersy, A. E. Abdelwahab, S. S. Abouelkhiir, D. M. Abou-Zeid and S. A. Sabry, *J. Basic Microbiol.*, 2012, **52**, 513–522.



- 4 A. K. Pandey and A. Kumar, *Process Biochem.*, 2014, **49**, 496–505.
- 5 K. Yamanaka, Y. Hamano and T. Oikawa, *J. Biosci. Bioeng.*, 2020, **129**, 558–564.
- 6 S. B. Bankar, S. A. Chaudhary and R. S. Singhal, *J. Sci. Ind. Res. India*, 2014, **73**, 33–40.
- 7 M. Zhu, Z. Zhang, Y. Liu, F. Wang, L. Xia, J. Xia and H. Guo, *Int. J. Polym. Sci.*, 2016, 3785036.
- 8 J. Chen, H. Liu, Z. Xia, X. Zhao, Y. Wu and M. An, *Molecules*, 2019, **24**, 1156.
- 9 X. S. Chen, K. F. Wang, G. C. Zheng, Y. Gao and Z. G. Mao, *Process Biochem.*, 2018, **68**, 22–29.
- 10 X. S. Chen, Q. Li, H. G. He, J. H. Zhang and Z. G. Mao, *RSC Adv.*, 2019, **9**, 12174–12181.
- 11 H. Katano, K. Uematsu, C. Maruyama and Y. Hamano, *Anal. Sci.*, 2014, **30**, 17–24.
- 12 H. Katano, Y. Kasahara, K. Ushimaru, C. Maruyama and Y. Hamano, *Anal. Sci.*, 2015, **31**, 1273–1277.
- 13 S. Li, Z. Ding, J. Liu and X. Cao, *Appl. Biochem. Biotech.*, 2017, **183**, 1254–1264.
- 14 A. L. Grilo, M. Raquel Aires-Barros and A. M. Azevedo, *Sep. Purif. Rev.*, 2016, **45**, 68–80.
- 15 P. L. Show, C. W. Ooi, M. S. Anuar, A. Ariff, Y. A. Yusof, S. K. Chen, M. S. M. Annuar and T. C. Ling, *Sep. Purif. Technol.*, 2013, **110**, 112–118.
- 16 Y. K. Lin, C. W. Ooi, J. S. Tan, P. L. Show, A. Ariff and T. C. Ling, *Sep. Purif. Technol.*, 2013, **120**, 362–366.
- 17 S. C. Lo, R. N. Ramanan, B. T. Tey, W. S. Tan, P. L. Show, T. C. Ling and C. W. Ooi, *Sep. Purif. Technol.*, 2018, **192**, 130–139.
- 18 P. Mathiazakan, S. Y. Shing, S. S. Ying, H. K. Kek, M. S. Tang, P. L. Show, C. W. Ooi and T. C. Ling, *Sep. Purif. Technol.*, 2016, **171**, 206–213.
- 19 Z. Li, H. Teng and Z. Xiu, *Process Biochem.*, 2010, **45**, 731–737.
- 20 C. A. E. Costa, P. C. R. Pinto and A. E. Rodrigues, *Sep. Purif. Technol.*, 2018, **192**, 140–151.
- 21 Z. Xu, Z. Xu, X. Feng, D. Xu, J. Liang and H. Xu, *Appl. Microbiol. Biotechnol.*, 2016, **100**, 6619–6630.
- 22 Y. Wang, Y. Liu, J. Han and S. Hu, *Sep. Sci. Technol.*, 2011, **46**, 1283–1288.
- 23 C. W. Ooi, B. T. Tey, S. L. Hii, S. M. M. Kamal, J. C. W. Lan, A. B. Ariff and T. C. Ling, *Process Biochem.*, 2009, **44**, 1083–1087.
- 24 J. Hiraki, T. Ichikawa, S. Ninomiya, H. Seki, K. Uohama, H. Seki, S. Kimura, Y. Yanagimoto and J. W. Barnett Jr, *Regul. Toxicol. Pharmacol.*, 2003, **37**, 328–340.
- 25 X. S. Chen, Y. Gao, B. Zhen, D. Han, J. H. Zhang and Z. G. Mao, *Process Biochem.*, 2016, **51**, 134–141.
- 26 T. Tan, Q. Huo and Q. Ling, *Biotechnol. Lett.*, 2002, **24**, 1417–1420.
- 27 F. R. Itzhaki, *Anal. Biochem.*, 1972, **50**, 569–574.
- 28 P. Kahar, T. Iwata, J. Hiraki, E. Y. Park and M. Okabe, *J. Biosci. Bioeng.*, 2001, **91**, 190–194.
- 29 B. Zhen, X. S. Chen, D. Han and Z. G. Mao, *Food and Bioprod. Process.*, 2015, **95**, 332–338.
- 30 M. Nishikawa, *Enzyme Microb. Tech.*, 2009, **45**, 295–298.

